Atmos. Chem. Phys. Discuss., 13, 29413–29445, 2013
www.atmos-chem-phys-discuss.net/13/29413/2013/
doi:10.5194/acpd-13-29413-2013

Atmospheric Chemistry and Physics Discussions

Atmospheric black carbon can exhibit enhanced light absorption at high relative humidity

Y. Wei, Q. Zhang, and J. E. Thompson

Texas Tech University, Lubbock, Texas, USA

Received: 24 October 2013 – Accepted: 29 October 2013 – Published: 11 November 2013

Correspondence to: J. E. Thompson (jon.thompson@ttu.edu)

Published by Copernicus Publications on behalf of the European Geosciences Union.

Abstract

Some estimates suggest atmospheric soot (a.k.a. black carbon, BC) warms Earth's climate by roughly 50 % the magnitude of increased carbon dioxide. However, one uncertainty in the climate-forcing estimate for BC is the degree to which sunlight absorption is influenced by particle mixing state. Here we show that hygroscopic growth of atmospheric aerosol particles sampled at Houston, TX leads to an enhancement in both light scattering and absorption. Measurements suggest light absorption increases roughly three-four fold at high ambient humidity for coated soot particles. However, when the fraction of coated BC particles was reduced, the absorption enhancement was also reduced, suggesting coatings are crucial for the effect to occur. In addition, the extent to which MAC was increased at high humidity varied considerably over time, even for BC that consistently presented as being coated. This suggests the chemical composition of the coating and/or source of BC may also be an important parameter to constrain MAC enhancement at high humidity. Nonetheless, the results are largely consistent with previous laboratory and model results predicting absorption enhancement. We conclude that the enhanced absorption increases the warming effect of soot aerosol aloft, and global climate models should include parameterizations for RH effects to accurately describe absorptive heating by BC.

1 Introduction

Black carbon (BC; a.k.a. soot) aerosol present in earth's atmosphere is believed to exert a positive direct radiative forcing (DRF) on Earth's climate between +0.08–1.27 $W m^{-2}$ due to its efficient light absorbing nature (Bond et al., 2013). This estimate suggests BC is the second most important climate-forcing agent behind long-lived greenhouse gases. However, the degree to which BC warms the Earth-atmosphere system is intimately linked to the efficiency with which soot absorbs sunlight. The mass absorption cross section (MAC, $m^2 g^{-1}$) is commonly used to relate absorption of light

ACPD
13, 29413–29445, 2013

to BC mass loading. The MAC is defined here as the ratio between the aerosol absorption coefficient (b_{abs}, Mm^{-1}) and the BC mass concentration ($\mu g\,m^{-3}$).

$$\text{M.A.C.} = \frac{b_{abs}}{[BC]}. \quad (1)$$

One uncertainty in constraining DRF by BC is assigning accurate MAC values. A review of theory and literature has led Bond and Bergstrom (2006) to report a MAC for fresh BC between 4–8 $m^2\,g^{-1}$. However, it is well known that BC quickly becomes internally mixed (embedded or coated) within other materials including hygroscopic sulfates, nitrates, and organics once released into the atmosphere (Cheng et al., 2012; Laborde 2013; Liu, 2013, 2010; Matsui, 2013; Metcalf et al., 2012; Moffet and Prather 2009; Moteki et al., 2007; Niu et al., 2007; Schwarz et al., 2006, 2008; Shiraiwa et al., 2007; Adachi and Buseck, 2008, 2013). Internal mixing of soot increases its ability to uptake water at high humidity (fresh uncoated soot is not hygroscopic) and both light scattering theory and laboratory measurements suggest the MAC value increases when BC becomes coated during atmospheric processing (Bond et al., 2006; Bueno et al., 2011; Khalizov et al., 2009; Lack et al., 2009; Liu et al., 2012; Mikhailov et al., 2006; Nessler et al., 2005; Saathoff, et al., 2003; Schnaiter et al., 2003, 2005; Shiraiwa et al., 2010; Xue et al., 2009; Wei et al., 2013). Bond et al. (2006) and Fuller et al. (1999) have postulated absorption enhancement factors of 2–5 fold were reasonable for thickly coated BC, however, attempts to measure absorption enhancement for dried atmospheric aerosols sampled in California found very modest enhancements (Cappa et al., 2012; Thompson et al., 2012). More recent data collected in Europe has suggested higher absorption enhancements (roughly 40 %) for coated atmospheric BC (Liu et al., 2013). These results suggest significant differences may exist between locations as has been suggested by Jacobson (2013). At present, it is believed the discrepancy between expected results and ambient samples results from BC cores in the dried, authentic samples not exhibiting a core-shell geometry necessary to observe large absorption enhancements. However, formation of an aqueous phase at high relative humidity (RH) may allow the light absorbing inclusions to be located at random

ACPD
13, 29413–29445, 2013

locations within a spherical droplet, thereby allowing enhanced absorption to occur. Since water vapor is by far the most abundant, easily condensed species in Earth's atmosphere it is reasonable to explicitly study the absorption enhancement phenomenon as a function of relative humidity. The condensation of water into a BC containing particle would provide sufficient mass to grow thick coatings required for largest absorption enhancement. Increased absorption by coated soot at high RH may help explain recent observations from China of increased solar heating rates aloft when BC was mixed with sulfate aerosol (Ramana, 2010) or allow additional understanding of enhanced absorption within clouds (Ramanathan, 1997). Therefore, results presented within this manuscript have significant impact on modeling both direct and indirect mechanisms of climate forcing. Yet, future measurements at additional times and locations are required to build a more comprehensive data set.

2 Experimental methods

A schematic of the experimental setup for ambient aerosol measurement is shown in Fig. 1.

2.1 Sampling conditions

Aerosol sampling occurred in an urban area within Houston TX (Lat: 29.685741, Long:-95.295668) from 19–24 July 2013. The location was 4–5 km NNW of William P. Hobby airport and was located at a Texas Commission on Environmental Quality (TCEQ) monitoring site (CAMS 416). During sampling outdoor temperatures ranged from 23.9–33.3 °C with a relative humidity range of 45–90 %. Winds were generally $< 16\,\mathrm{km\,h^{-1}}$ and frequently from the south or southeast. Aerosol was sampled at 3–4 LPM into a 3 m long length of 1.25 cm inner diameter copper tube without size selection and passed through a window into a climate-controlled building where the measurement devices were located. The tubing inlet was approx. 4 m a.g.l. Temperature within the

ACPD
13, 29413–29445, 2013

building was 23.6 ± 3 °C, and the drop in temperature was used to promote high values of relative humidity for the sample. Flow through the copper tube was split at a 1/2″ Swagelok tee ("first tee" in Fig. 1). One arm of the tee was routed to a diffusion dryer (TSI 3062 with silica gel/Drierite dessicant) to lower the sample humidity and then to an electronic 3-way ball valve (Assured Automation, EV1S1V1) that was actuated under computer control. The second line from the mixing tee (e.g. wet-air-line) was routed directly to the electronic valve with a 1 m length of 0.93 cm diameter conductive rubber tubing (TSI Inc.). The common port of the electronic valve was connected to the albedometer with a 2.5 m length of 0.93 cm diameter conductive rubber tubing. Cycling the electronic valve every 15–30 min under computer control allowed sequential probing of wet and dried ambient aerosol.

2.2 Measurements

Measurements of aerosol scattering, extinction, and absorption coefficients (b_{scat}, b_{ext}, b_{abs}; Mm^{-1}) were carried out using the aerosol albedometer as described in previous literature (Thompson et al., 2008; Dial et al., 2010; Redmond et al., 2011; Ma et al., 2012). Scattering calibration occurred against R-134a (Zadoo and Thompson, 2011) as typical for the experiment. Sample relative humidity was measured at the outlet of the albedometer optical cell with a Vaisala HMP 60 sensor. Uncertainty in this RH sensor is specified to be +5 %. While the aerosol albedometer offers improved truncation performance for nephelometry, size dependent corrections to b_{scat} on the order of a few percent are often necessary. To correct the optical data at high RH, a hygroscopic growth model must be used to estimate aerosol diameters and truncation effects considered. Qian et al. (2012) developed a correction scheme for the albedometer b_{scat} measurement based on particle size parameter that we have employed to correct data. The hygroscopic growth model used was developed from a combination of observational data from the literature, and the AIM thermodynamic model (http://www.aim.env.uea.ac.uk/aim/aim.php). Growth factors as a function of relative humidity are illustrated in Fig. 2. The model used (red data points) seeks the

ACPD
13, 29413–29445, 2013

median of observational data at RH values below 90 %. Since observational data was not frequently available at RH > 90 %, we assumed hygroscopic growth consistent with ammonium sulfate at very high RH. Assuming the aerosol behaves as such may overestimate hygroscopic growth above 90 % RH. Overestimating hygroscopic growth via this model would lead to smaller values of absorption and consequently smaller M.A.C. This encourages a conservative estimate of MAC increase at high RH.

The SP2-D Single Particle Soot Photometer was also plumbed into the setup immediately after the albedometer to monitor rBC mass concentration and mixing state. The SP2 purge flow was filtered dry air. During field measurements, the SP2 was configured to save data for between 1 of 5 and 1 of 20 particles observed. The instrument was also periodically configured to collect/save data only 1 of 5 min. Both of these conditions were used to save hard drive space on the instrument (accumulates GB of data daily), but assuming random sampling this should not affect results. After the field campaign, the SP2 was calibrated in the laboratory against atomized, and size selected fullerene soot (Alfa Aesar) and SP2 indicated diameters agreed well with electrostatic selection diameters as shown in Fig. A1 of the Appendix. The Probe Analysis Package for Igor (PAPI) provided by DMT was used for data analysis of SP2 data. The dry-air sampling line also included a sampling port for a Droplet Measurement Technologies (PAX) Photoacoustic Extinctiometer (also measures b_{abs} and b_{scat}) that sampled the dry aerosol at 1 LPM.

3 Results and discussion

3.1 BC mixing state analysis

Incandescence lag time analysis was used to probe BC mixing state from raw SP2 data. The approach we used was highly influenced by previous literature (Schwarz et al., 2006; Subramanian et al., 2010; Moteki et al., 2007; Shiraiwa et al., 2007). For the current analysis an incandescence lag time delay of 1 µs was used as a criteria

ACPD
13, 29413–29445, 2013

to determine whether a BC containing particle was uncoated or coated. Here, lag time delay is defined as the difference between peak incandescence signal and peak elastic scatter signal indicated by the SP-2. The lag time delay is believed to result from time required to evaporate non-refractory materials from the BC containing particle as it heats in the laser beam. To justify the choice of a 1 µs delay, we present the results of Fig. 3. This figure illustrates plots of scatter – to – incandescence peak ratio vs. lag time for a variety of laboratory generated test aerosols of known mixing state. The panel on the bottom left is for dry, uncoated kerosene soot. Virtually all particles (denoted by data points) exhibited lag times < 1 µs. However, when kerosene soot was collected and atomized from suspensions containing either ammonium sulfate, ammonium nitrate, or glycerol the observed lag times increased – generally to > 1 µs. The increase in scatter/incandescence peak ratio observed is also consistent with the particles being coated. Clearly, the data reflects 1 µs lag time is a good threshold to describe BC coat state. Thus, individual particles measured in Houston were assigned to either being "coated" or "not coated" based on observed lag time – no distinction was made as to the thickness of coating present. Therefore, the coating fraction is defined as the fraction of particles exhibiting a lag time of > 1 µs.

3.2 BC size and mass concentration

As observed in Fig. 4a, the daily modes of the mass-equivalent diameter distributions of BC cores sensed by the SP2 were consistently near Dp = 120 nm. Figure 4b illustrates time series plots of rBC mass concentration and coating fraction as well as histograms of observed results. The mass concentration of rBC was between 33 and 5340 ng m^{-3} during the sampling period with an average of 682 ng m^{-3}. The coating fraction varied between approx. 0.2–0.9 with a mean of 0.68. The coating fraction often dropped when concentrated plumes of rBC passed the sampling site. Both results are consistent with local sources being responsible for fresh emissions within very concentrated plumes.

ACPD
13, 29413–29445, 2013

3.3 Optical measurement results

The mean aerosol absorption, scatter, and extinction coefficients observed on dry aerosol (< 60 % RH) sampled at the Houston site are summarized in Table 1. As reported in the table, mean absorption and scattering coefficients were fairly low compared to measurements from other urban environments. However, the mean $PM_{2.5}$ mass concentration reflected in the TEOM data, and presented in Table 1 agreed closely with measurements from July 2010–2012 (13.24, 10.71, 14.46 $\mu g\,m^{-3}$, respectively) suggesting we may have experienced similar aerosol mass loadings despite the limited sampling period.

Figure 5 illustrates a plot of mass scatter coefficient ($b_{scat}/PM_{2.5}$ mass concentration; $m^2\,g^{-1}$) vs. sample relative humidity for the Houston data set. Each data point on the graph was a five minute average obtained by dividing the optical measurement by the associated mass concentration. $PM_{2.5}$ mass concentration was determined via an automated TEOM instrument located within 100 m of the sampling site (operated by TCEQ). As observed in Fig. 5, the mass scatter coefficient was found to increase dramatically when sample RH was > 75 %. This enhanced scattering at high RH is a well-known phenomenon (see ten Brink et al., 2000; Carrico et al., 1998; Cropper et al., 2013; Kus et al., 2004; Liu et al., 2012 and references within).

We also report measurements of soot MAC ($m^2\,g^{-1}$) for aerosol sampled at Houston, TX that exhibit significant absorption enhancement at elevated relative humidity. Furthermore, the absorption enhancement was, on average, affected by the mixing/coating fraction of the BC. Figure 6 illustrates data showing the effect of relative humidity on aerosol optics. Again, aerosol was sampled through an inlet that cycled between low and high relative humidity (RH). Water vapor condensed into hygroscopic materials at high RH causing deliquescence of particles and formation of internally mixed aerosol consisting of an aqueous phase and BC of ≈ 120 nm mass equivalent diameter. As illustrated in the figure, cycles of high humidity yielded clear increases in aerosol scattering coefficient (b_{scat}). Indicated aerosol absorption coefficient (b_{abs}) also

ACPD
13, 29413–29445, 2013

often increased during cycles of high RH despite mass concentrations of BC remaining relatively constant. This is easiest observed within the middle portion of Fig. 6a. Figure 6b illustrates data collected during the morning hours of 24 July. Prior to 450 ks BC aerosol was fairly dilute and was highly coated. During this first period, cycling of MAC in phase with RH was observed. As local traffic/activities increased during the morning commute (beginning at approx. 450 ks), additional fresh BC was added to the local atmosphere and the fraction of BC coated was observed to drop. Simultaneously, it became difficult to detect a large MAC increase at high humidity. This result may be expected since uncoated BC is generally not hygroscopic. However, the differences in MAC enhancement observed between panels 6a and 6b suggest that the chemical composition, phase, viscosity or other property of the BC coating likely affects MAC alteration at high RH.

The image plot depicted in Fig. 7 illustrates observed MAC values as a function of RH and coating fraction for all data collected during the sampling period 19–24 July 2013. MAC values in excess of $20\,m^2\,g^{-1}$ were indicated at high RH when a large fraction of BC was coated. Also illustrated within inset B. of Fig. 7 are median MAC values plotted against RH for low (< 0.5), medium (0.5–0.75), and high coat (> 0.75) state conditions. The error bars in the graph represent 25–75 % tiles. As observed, median MAC increased from approx. 4 to $15\,m^2\,g^{-1}$ as humidity increased from 50–95 % for BC samples exhibiting coat fractions of > 0.75. Such a dramatic increase in MAC was not observed when BC coating fraction was < 0.5, although medians still exhibited a ≈ 50 % increase – even in this case. We attribute this increase to the minority coated BC fraction present. Inset A of Fig. 7 presents a plot of observed MAC as a function of coating fraction when sample RH was < 60 %. Interestingly, the median MAC values increased only marginally from 3.8 to $4.4\,m^2\,g^{-1}$ as median BC coating fraction increased from 0.47–0.78. This small increase (c.a. 15 %) could be the result of optical lensing by non-absorbing coatings, but the magnitude of increase in MAC for dried aerosol coatings appears to be small compared to that encountered through RH effects. This result is largely consistent with the marginal absorption enhancement recently re-

ACPD
13, 29413–29445, 2013

ported by Cappa et al. (2012) and Thompson et al. (2012) for dried aerosols sampled in California. The increased MAC values at high humidity observed in Fig. 7 are also consistent with modeled projections of 2–5 fold absorption enhancement advocated by Bond et al. (2006) and Fuller et al. (1999) for light absorbing BC inclusions located randomly within non-absorbing shells. The 3–4 fold enhancement in MAC observed at high RH also agrees very well with the laboratory work of Mikhailov et al. (2006), who observed an absorption enhancement for laboratory generated hydrophilic soot aerosols of 3–4 fold. In addition, results are similar to the enhancement observed by Wei et al. (2013) for lab generated soot particles internally mixed with sulfate. The highest measurements of MAC observed corresponded to time periods in which the concentration of BC and b_{abs} was low, and RH was high. If any positive offset bias (incorrect zero measurement) exists in the measurements, it would lead to falsely high MAC values, particularly at low concentrations of BC. In addition, the periods of low BC concentration and low b_{abs} will be prone to the highest relative uncertainty in MAC. Figure A4 reports propagated absolute uncertainty in MAC using absolute uncertainties of 2 Mm^{-1} for absorption and 50 $ng\,m^{-3}$ for [BC]. As observed, uncertainty was not constant through the rBC coat fraction and RH space defined in Fig. 7. This is because high coat fraction tended to be observed for very dilute, aged BC plumes. This uncertainty should be considered a caveat of the data set. However, an analysis conducted using only data when [BC] > 0.5 $\mu g\,m^{-3}$ also yielded a 3–4 fold increase of MAC. Also, significant increases in indicated aerosol absorption were also evident in the time-series data upon cycling to high RH without recalibrating step, so positive offset error is likely not to blame for all results. Finally, plots of indicated absorption vs. mass concentration of BC for low RH and high RH subdivisions of the data set yielded different slopes for best-fit lines (slope is MAC). Therefore, we can be confident the MAC enhancement truly exists. However, setting specific quantitative bounds on the enhancement factor remains challenging.

ACPD
13, 29413–29445, 2013

3.3.1 Mechanism of enhanced absorption

Organic compounds present in certain aerosol samples can also absorb visible light (Lukacs et al., 2007; Shapiro et al., 2009; Chang and Thompson, 2010). To evaluate whether such compounds were present and could influence results, we collected particles onto a filter and extracted the material with a 20 : 80 v/v mix of methanol and water. The extracts were filtered through a syringe filter to remove insoluble materials and measured using a standard UV-VIS spectrophotometer and a 1 cm path length cell. Figure A2 of the appendix displays several spectra of the extracts (colored traces) from different dates/times. In addition, a spectroscopic blank taken at the conclusion of analysis is shown in black. The filter extracts exhibited substantial absorption in the near UV between 300–400 nm, but very little or no light absorption in the visible spectral region. Also, back trajectory analysis (Fig. A3) indicates the sampled air masses originated from over the Gulf of Mexico during the sampling period, a region not heavily influenced by biomass combustion. We conclude brown-colored carbon containing compounds are not responsible for increases in MAC at high RH observed at 532 nm.

Alternatively, light absorption by BC can be enhanced when BC is fully immersed within an aqueous droplet here called "core-shell model") or when BC is present on the droplet's surface (here called the "sphere-on-sphere model"). Figure 8a illustrates the electric field within and near a 2 micron diameter water droplet (normalized to incident field = 1) as modeled with the ADDA discrete dipole code (Yurkin and Hoesktra, 2011). As observed the internal electric field within the droplet can exceed the incident field (approx. double at many locations). In addition, the largest enhancement occurs within a small volume directly adjacent to the particle on the "shaded side" (e.g. in the optical near-field of the particle). Field enhancements > 10 fold can be encountered in this region, and soot MAC values > 100 $m^2 g^{-1}$ are modeled when a soot particle resides within this volume. However, we would expect a soot particle to randomly occupy all volume elements on the surface of the droplet for the sphere-on-sphere model, and orientation averaging is required to describe the enhancement for this non-symmetrical

ACPD
13, 29413–29445, 2013

case. The results of Fig. 8b report modeled MAC values for the core-shell and sphere-on-sphere models using ADDA. As observed, orientation averaging reduces the average absorption enhancement predicted for the sphere-on-sphere case. In fact, after orientation averaging, the mean enhancement expected for the sphere on sphere model is less than the core-shell case. MAC values in the range of 15–20 $m^2 g^{-1}$ can only be modeled via the core-shell approach. Therefore, the measurement results presented in Fig. 7 agree best with the core-shell model. However, we feel the exact physical mechanism by which the absorption enhancement is achieved is still open to further investigation. Given the uncertainty reported in Fig. A4, we cannot completely discount the sphere-on-sphere model (or an alternate model) is producing the enhancement. Attempts to immerse soot within aqueous phases in our laboratory have largely been unsuccessful despite considerable efforts to chemically modify the soot particle surface (e.g. make surface more hydrophilic) by treatment with ozone, nitric acid vapor, natural surfactants, inorganic salts, and combinations of these. Experiments aimed at imaging soot mixed with aerosolized droplets are needed to confirm the "core-shell" morphology. In addition, more measurements of absorption enhancement at high RH for a variety of locations globally are definitely needed to bring this issue to scientific closure. The chemical composition of soot coatings should simultaneously be tracked to better understand why soot exhibits large MAC enhancements at high RH during certain periods of time, and very little enhancements during others (as in Fig. 6).

4 Significance and conclusion

The measurement results described within provide evidence for significant absorption enhancement by coated BC aerosol at high humidity. Since BC becomes coated in the atmosphere within 3–5 h of release, this experimental result suggests climate models should include parameterizations that account for increased absorption by soot aerosol at high relative humidity as advocated by Jacobson (2012). If parameterizations are not included, the actual direct radiative forcing by soot aerosol may be > 100 % more posi-

ACPD
13, 29413–29445, 2013

tive. While Fig. 7 may provide some initial quantitative guidance, we recognize multiple caveats to our experiment. Given the uncertainties associated with our measurements, we are unable to assess whether core-shell or sphere-on-sphere morphologies are most representative of reality. In addition, the "correct" model may depend on the composition of coating or soot surface chemistry. Data shows the magnitude of increase in MAC observed at high humidity clearly varied in time. For some sampling periods, almost no enhancement at high RH was observed, while during others MAC values increased by > 4-fold. This suggests the chemical composition of coatings or the soot source may be important factors to model absorption enhancement at high RH. A more comprehensive characterization of the composition of soot coating material is required to gain additional insights on absorption enhancement at high RH.

Supplementary material related to this article is available online at http://www.atmos-chem-phys-discuss.net/13/29413/2013/acpd-13-29413-2013-supplement.pdf.

Acknowledgements. Development of the albedometer was historically funded by the National Science Foundation. We thank P. Beltz, City of Houston Environmental Health for hosting us during measurements. We are also grateful to G. McMeeking and Droplet Measurement Technologies for providing a SP2-D for measurements. We are also grateful to Fernando Mercado of TCEQ for providing high time resolution $PM_{2.5}$ data for the site.

References

Adachi, K. and Buseck, P. R.: Internally mixed soot, sulfates, and organic matter in aerosol particles from Mexico City, Atmos. Chem. Phys., 8, 6469–6481, doi:10.5194/acp-8-6469-2008, 2008.

Adachi, K. and Buseck, P. R.: Changes of ns-soot mixing states and shapes in an urban area during CalNex, J. Geophys. Res.-Atmos., 118, 3723–3730, doi:10.1002/Jgrd.50321, 2013.

ACPD
13, 29413–29445, 2013

Bond, T. and Bergstrom, R.: Light absorption by carbonaceous particles: an investigative review, Aerosol Sci. Tech., 40, 27–67, doi:10.1080/02786820500421521, 2006.
Bond, T., Habib, G., and Bergstrom, R.: Limitations in the enhancement of visible light absorption due to mixing state, J. Geophys. Res.-Atmos., 111, D20211, doi:10.1029/2006JD007315, 2006.
Bond, T. C., Doherty, S. J., Fahey, D. W., Forster, P. M., Berntsen, T., DeAngelo, B. J., Flanner, M. G., Ghan, S., Kärcher, B., Koch, D., Kinne, S., Kondo, Y., Quinn, P. K., Sarofim, M. C., Schultz, M. G., Schulz, M., Venkataraman, C., Zhang, H., Zhang, S., Bellouin, N., Guttikunda, S. K., Hopke, P. K., Jacobson, M. Z., Kaiser, J. W., Klimont, Z., Lohmann, U., Schwarz, J. P., Shindell, D., Storelvmo, T., Warren, S. G., and Zender, C. S.: Bounding the role of black carbon in the climate system: a scientific assessment, J. Geophys. Res.-Atmos., 118, 5380–5552, 2013.
Bueno, P. A., Havey, D. K., Mulholland, G. W., Hodges, J. T., Gillis, K. A., Dickerson, R. R., and Zachariah, M. R.: Photoacoustic measurements of amplification of the absorption cross section for coated soot aerosols, Aerosol Sci. Tech., 45, 1217–1230, doi:10.1080/02786826.2011.587477, 2011.
Cappa, C. D., Onasch, T. B., Massoli, P., Worsnop, D. R., Bates, T. S., Cross, E. S., Davidovits, P., Hakala, J., Hayden, K. L., Jobson, B. T., Kolesar, K. R., Lack, D. A., Lerner, B. M., Li, S.-M., Mellon, D., Nuaaman, I., Olfert, J. S., Petaja, T., Quinn, P. K., Song, C., Subramanian, R., Williams, E. J., and Zaveri, R. A.: Radiative absorption enhancements due to the mixing state of atmospheric black carbon, Science, 337, 1078–1081, 2012.
Carrico, C. M., Rood, M. J., and Ogren, J. A.: Aerosol light scattering properties at Cape Grim, Tasmania, during the First Aerosol Characterization Experiment (ACE 1), J. Geophys. Res.-Atmos., 103, 16565–16574, doi:10.1029/98jd00685, 1998.
Chang, J. and Thompson, J.: Characterization of colored products formed during irradiation of aqueous solutions containing H_2O_2 and phenolic compounds, Atmos. Environ., 44, 541–551, doi:10.1016/j.atmosenv.2009.10.042, 2010.
Cheng, Y. F., Su, H., Rose, D., Gunthe, S. S., Berghof, M., Wehner, B., Achtert, P., Nowak, A., Takegawa, N., Kondo, Y., Shiraiwa, M., Gong, Y. G., Shao, M., Hu, M., Zhu, T., Zhang, Y. H., Carmichael, G. R., Wiedensohler, A., Andreae, M. O., and Pöschl, U.: Size-resolved measurement of the mixing state of soot in the megacity Beijing, China: diurnal cycle, aging and parameterization, Atmos. Chem. Phys., 12, 4477–4491, doi:10.5194/acp-12-4477-2012, 2012.

ACPD
13, 29413–29445, 2013

Cropper, P. M., Hansen, J. C., and Eatough, D. J.: Measurement of light scattering in an urban area with a nephelometer and $PM_{2.5}$ FDMS TEOM monitor: accounting for the effect of water, J. Air Waste Manage., 63, 1004–1011, doi:10.1080/10962247.2013.770421, 2013.

Fuller, K. A., Malm, W. C., and Kreidenweis, S. M.: Effects of mixing on extinction by carbonaceous particles, J. Geophys. Res.-Atmos., 104, 15941–15954, doi:10.1029/1998JD100069, 1999.

Jacobson, M. Z.: Investigating cloud absorption effects: Global absorption properties of black carbon, tar balls, and soil dust in clouds and aerosols, J. Geophys. Res.-Atmos., 117, D06205, doi:10.1029/2011jd017218, 2012.

Jacobson, M. Z.: Comment on "Radiative Absorption Enhancements Due to the Mixing State of Atmospheric Black Carbon", Science, 339, p. 393, doi:10.1126/science.1229920, 2013.

Khalizov, A. F., Xue, H. X., Wang, L., Zheng, J., and Zhang, R. Y.: Enhanced Light Absorption and Scattering by Carbon Soot Aerosol Internally Mixed with Sulfuric Acid, J. Phys. Chem. A, 113, 1066–1074, doi:10.1021/Jp807531n, 2009.

Kus, P., Carrico, C. M., Rood, M. J., and Williams, A.: Measured and modeled light scattering values for dry and hydrated laboratory aerosols, J. Atmos. Ocean. Tech., 21, 981–994, doi:10.1175/1520-0426(2004)021<0981:mamlsv>2.0.co;2, 2004.

Laborde, M., Crippa, M., Tritscher, T., Jurányi, Z., Decarlo, P. F., Temime-Roussel, B., Marchand, N., Eckhardt, S., Stohl, A., Baltensperger, U., Prévôt, A. S. H., Weingartner, E., and Gysel, M.: Black carbon physical properties and mixing state in the European megacity Paris, Atmos. Chem. Phys., 13, 5831–5856, doi:10.5194/acp-13-5831-2013, 2013.

Lack, D. A., Cappa, C. D., Cross, E. S., Massoli, P., Ahern, A. T., Davidovits, P., and Onasch, T. B.: Absorption enhancement of coated absorbing aerosols: validation of the photo-acoustic technique for measuring the enhancement, Aerosol Sci. Tech., 43, 1006–1012, doi:10.1080/02786820903117932, 2009.

Liu, C., Panetta, R. L., and Yang, P.: The influence of water coating on the optical scattering properties of fractal soot aggregates, Aerosol Sci. Tech., 46, 31–43, doi:10.1080/02786826.2011.605401, 2012.

Liu, D., Flynn, M., Gysel, M., Targino, A., Crawford, I., Bower, K., Choularton, T., Jurányi, Z., Steinbacher, M., Hüglin, C., Curtius, J., Kampus, M., Petzold, A., Weingartner, E., Baltensperger, U., and Coe, H.: Single particle characterization of black carbon aerosols at a tropospheric alpine site in Switzerland, Atmos. Chem. Phys., 10, 7389–7407, doi:10.5194/acp-10-7389-2010, 2010.

ACPD
13, 29413–29445, 2013

Liu, D., Allan, J., Whitehead, J., Young, D., Flynn, M., Coe, H., McFiggans, G., Fleming, Z. L., and Bandy, B.: Ambient black carbon particle hygroscopic properties controlled by mixing state and composition, Atmos. Chem. Phys., 13, 2015–2029, doi:10.5194/acp-13-2015-2013, 2013.

Liu, S., Aiken, A. C., Gorkowski, K., Dubey, M., Herndon, S., Williams, L., Massoli, P., Fortner, E., Freedman, A., Worsnop, D. R., Ng, N. L., Mohr, C., Lopez-Hilfiker, F., Thornton, J., Allan, J., and Cappa, C. D.: Enhanced Light Absorption by Internally Mixed Atmospheric Black Carbon in Europe, 32nd Annual Conference AAAR, 393, 2013.

Liu, X. G., Zhang, Y. H., Cheng, Y. F., Hu, M., and Han, T. T.: Aerosol hygroscopicity and its impact on atmospheric visibility and radiative forcing in Guangzhou during the 2006 PRIDE-PRD campaign, Atmos. Environ., 60, 59–67, doi:10.1016/j.atmosenv.2012.06.016, 2012.

Lukacs, H., Gelencser, A., Hammer, S., Puxbaum, H., Pio, C., Legrand, M., Kasper-Giebl, A., Handler, M., Limbeck, A., Simpson, D., and Preunkert, S.: Seasonal trends and possible sources of brown carbon based on 2 yr aerosol measurements at six sites in Europe, J. Geophys. Res.-Atmos., 112, D23S18, doi:10.1029/2006jd008151, 2007.

Ma, L. and Thompson, J.: Optical properties of dispersed aerosols in the near ultraviolet (355 nm): measurement approach and initial data, Anal. Chem., 84, 5611–5617, doi:10.1021/ac3005814, 2012.

Massoli, P., Bates, T. S., Quinn, P. K., Lack, D. A., Baynard, T., Lerner, B. M., Tucker, S. C., Brioude, J., Stohl, A., and Williams, E. J.: Aerosol optical and hygroscopic properties during TexAQS-GoMACCS 2006 and their impact on aerosol direct radiative forcing, J. Geophys. Res.-Atmos., 114, D00F07, doi:10.1029/2008JD011604, 2009.

Matsui, H., Koike, M., Kondo, Y., Moteki, N., Fast, J. D., and Zaveri, R. A.: Development and validation of a black carbon mixing state resolved three-dimensional model: aging processes and radiative impact, J. Geophys. Res.-Atmos., 118, 2304–2326, doi:10.1029/2012jd018446, 2013.

Metcalf, A. R., Craven, J. S., Ensberg, J. J., Brioude, J., Angevine, W., Sorooshian, A., Duong, H. T., Jonsson, H. H., Flagan, R. C., and Seinfeld, J. H.: Black carbon aerosol over the Los Angeles Basin during CalNex, J. Geophys. Res.-Atmos., 117, D00V13, doi:10.1029/2011jd017255, 2012.

Mikhailov, E., Vlasenko, S., Podgorny, I., Ramanathan, V., and Corrigan, C.: Optical properties of soot-water drop agglomerates: an experimental study, J. Geophys. Res.-Atmos., 111, D07209, doi:10.1029/2005JD006389, 2006.

ACPD
13, 29413–29445, 2013

Moffet, R. C. and Prather, K. A.: In-situ measurements of the mixing state and optical properties of soot with implications for radiative forcing estimates, P. Natl. Acad. Sci. USA, 106, 11872–11877, doi:10.1073/Pnas.0900040106, 2009.

Moteki, N., Kondo, Y., Miyazaki, Y., Takegawa, N., Komazaki, Y., Kurata, G., Shirai, T., Blake, D. R., Miyakawa, T., and Koike, M.: Evolution of mixing state of black carbon particles: aircraft measurements over the western Pacific in March 2004, Geophys. Res. Lett., 34, L11803, doi:10.1029/2006gl028943, 2007.

Nessler, R., Weingartner, E., and Baltensperger, U.: Effect of humidity on aerosol light absorption and its implications for extinction and the single scattering albedo illustrated for a site in the lower free troposphere, J. Aerosol Sci., 36, 958–972, doi:10.1016/j.jaerosci.2004.11.012, 2005.

Niu, H. Y., Shao, L. Y., and Zhang, D. Z.: Aged status of soot particles during the passage of a weak cyclone in Beijing, Atmos. Environ., 45, 2699–2703, doi:10.1016/j.Atmosenv.2011.02.056, 2011.

Pan, X. L., Yan, P., Tang, J., Ma, J. Z., Wang, Z. F., Gbaguidi, A., and Sun, Y. L.: Observational study of influence of aerosol hygroscopic growth on scattering coefficient over rural area near Beijing mega-city, Atmos. Chem. Phys., 9, 7519–7530, doi:10.5194/acp-9-7519-2009, 2009.

Qian, F., Ma, L., and Thompson, J.: Modeling and measurements of angular truncation for an aerosol albedometer, J. Eur. Opt. Soc.-Rapid Publ., 7, 12021, doi:10.2971/jeos.2012.12021, 2012.

Ramana, M. V., Ramanathan, V., Feng, Y., Yoon, S.-C., Kim, S.-W., Carmichael, G. R., and Schauer, J. J.: Warming influenced by the ratio of black carbon to sulphate and the black-carbon source, Nat. Geosci., 3, 542–545, doi:10.1038/ngeo918, 2010.

Ramanathan, V. and Vogelmann, A. M.: Greenhouse effect, atmospheric solar absorption and the Earth's radiation budget: from the Arrhenius/Langley era to the 1990s., Ambio, 26, 38–46, 1997.

Redmond, H. and Thompson, J.: Evaluation of a quantitative structure–property relationship (QSPR) for predicting mid-visible refractive index of secondary organic aerosol (SOA), Phys. Chem. Chem. Phys., 13, 6872–6882, doi:10.1039/c0cp02270e, 2011.

Saathoff, H., Naumann, K. H., Schnaiter, M., Schock, W., Mohler, O., Schurath, U., Weingartner, E., Gysel, M., and Baltensperger, U.: Coating of soot and $(NH_4)_2SO_4$ particles by ozonolysis products of alpha-pinene, J. Aerosol Sci., 34, 1297–1321, doi:10.1016/S0021-8502(03)00364-1, 2003.

ACPD
13, 29413–29445, 2013

Santarpia, J. L., Gasparini, R., Li, R., and Collins, D.: Diurnal variations in the hygroscopic growth cycles of ambient aerosol populations, J. Geophys. Res.-Atmos., 110, D03206, doi:10.1029/2004JD005279, 2005.
Schnaiter, M., Horvath, H., Mohler, O., Naumann, K. H., Saathoff, H., and Schock, O. W.: UV-VIS-NIR spectral optical properties of soot and soot-containing aerosols, J. Aerosol Sci., 34, 1421–1444, doi:10.1016/S0021-8502(03)00361-6, 2003.
Schnaiter, M., Linke, C., Mohler, O., Naumann, K. H., Saathoff, H., Wagner, R., Schurath, U., and Wehner, B.: Absorption amplification of black carbon internally mixed with secondary organic aerosol, J. Geophys. Res.-Atmos., 110, D19204, doi:10.1029/2005jd006046, 2005.
Schwarz, J. P., Gao, R. S., Fahey, D. W., Thomson, D. S., Watts, L. A., Wilson, J. C., Reeves, J. M., Darbeheshti, M., Baumgardner, D. G., Kok, G. L., Chung, S. H., Schulz, M., Hendricks, J., Lauer, A., Karcher, B., Slowik, J. G., Rosenlof, K. H., Thompson, T. L., Langford, A. O., Loewenstein, M., and Aikin, K. C.: Single-particle measurements of midlatitude black carbon and light-scattering aerosols from the boundary layer to the lower stratosphere, J. Geophys. Res.-Atmos., 111, D16207, doi:10.1029/2006jd007076, 2006.
Schwarz, J. P., Gao, R. S., Spackman, J. R., Watts, L. A., Thomson, D. S., Fahey, D. W., Ryerson, T. B., Peischl, J., Holloway, J. S., Trainer, M., Frost, G. J., Baynard, T., Lack, D. A., de Gouw, J. A., Warneke, C., and Del Negro, L. A.: Measurement of the mixing state, mass, and optical size of individual black carbon particles in urban and biomass burning emissions, Geophys. Res. Lett., 35, L13810, doi:10.1029/2008gl033968, 2008.
Shapiro, E. L., Szprengiel, J., Sareen, N., Jen, C. N., Giordano, M. R., and McNeill, V. F.: Light-absorbing secondary organic material formed by glyoxal in aqueous aerosol mimics, Atmos. Chem. Phys., 9, 2289–2300, doi:10.5194/acp-9-2289-2009, 2009.
Shiraiwa, M., Kondo, Y., Moteki, N., Takegawa, N., Miyazaki, Y., and Blake, D. R.: Evolution of mixing state of black carbon in polluted air from Tokyo, Geophys. Res. Lett., 34, L16803, doi:10.1029/2007gl029819, 2007.
Shiraiwa, M., Kondo, Y., Iwamoto, T., and Kita, K.: Amplification of light absorption of black carbon by organic coating, Aerosol Sci. Tech., 44, 46–54, doi:10.1080/02786820903357686, 2010.
Swietlicki, E., Hansson, H. C., Hameri, K., Svenningsson, B., Massling, A., McFiggans, G., McMurry, P. H., Petaja, T., Tunved, P., Gysel, M., Topping, D., Weingartner, E., Baltensperger, U., Rissler, J., Wiedensohler, A., and Kulmala, M.: Hygroscopic properties of submicrometer at-

ACPD
13, 29413–29445, 2013

mospheric aerosol particles measured with H-TDMA instruments in various environments – a review, Tellus B, 60, 432–469, 2008.
ten Brink, H. M., Khlystov, A., Kos, G. P. A., Tuch, T., Roth, C., and Kreyling, W.: A high-flow humidograph for testing the water uptake by ambient aerosol, Atmos. Environ., 34, 4291–4300, doi:10.1016/s1352-2310(00)00197-7, 2000.
Thompson, J., Barta, N., Policarpio, D., and DuVall, R.: A fixed frequency aerosol albedometer, Opt. Express, 16, 2191–2205, doi:10.1364/OE.16.002191, 2008.
Thompson, J. E., Hayes, P. L., Jimenez, J. L., Adachi, K., Zhang, X., Liu, J., Weber, R. J., and Buseck, P. R.: Aerosol optical properties at Pasadena, CA during CalNex 2010., Atmos. Environ., 55, 190–200, doi:10.1016/j.atmosenv.2012.03.011, 2012.
Wei, Y., Ma, L., Cao, T., Zhang, Q., Wu, J., Buseck, P. R., and Thompson, J. E.: Light scattering and extinction measurements combined with laser-induced incandescence for the real-Time Determination of Soot Mass Absorption Cross Section, Anal. Chem., 85, 9181–9188, 2013.
Xue, H. X., Khalizov, A. F., Wang, L., Zheng, J., and Zhang, R. Y.: Effects of dicarboxylic acid coating on the optical properties of soot, Phys. Chem. Chem. Phys., 11, 7869–7875, doi:10.1039/B904129j, 2009.
Zadoo, S. and Thompson, J. E.: Rayleigh scattering measurements of several fluorocarbon gases, J. Environ. Monitor., 13, 3294–3297, 2011.

ACPD
13, 29413–29445, 2013

Table 1. Mean aerosol optical values observed at Houston, TX for dried aerosol (RH < 60 %) during 19–24 July 2013.

Parameter	Mean	25th %tile	75th %tile
Absorption, b_{abs}	2.9 Mm^{-1}	0.62	3.5
Scattering, b_{scat}	26.0 Mm^{-1}	22	31.7
Extinction, b_{ext}	28.9 Mm^{-1}	23.8	34.6
Albedo, SSA	0.91 Mm^{-1}	0.86	0.97
$PM_{2.5}$	13.0 $\mu g\,m^{-3}$	8.4	17.7

ACPD
13, 29413–29445, 2013

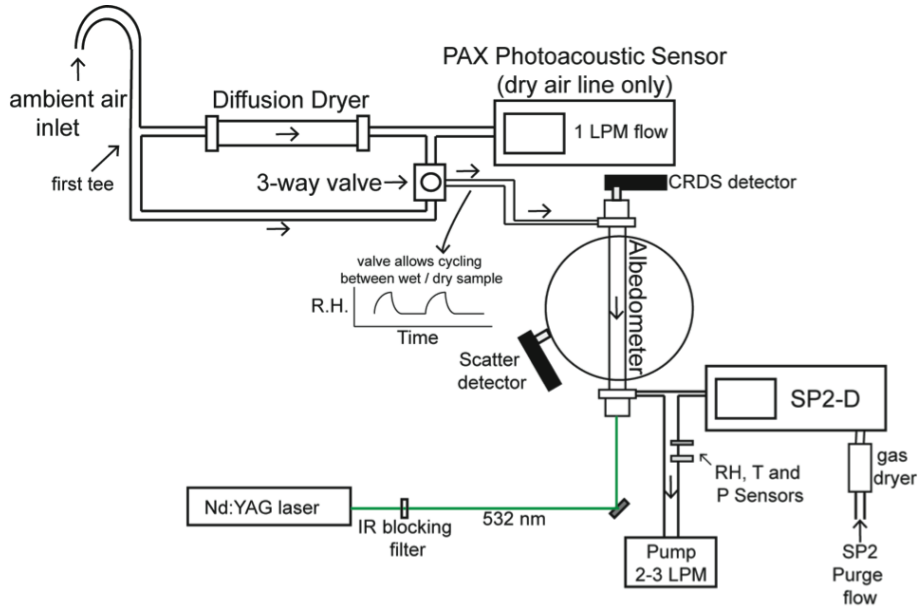

Fig. 1. Experimental setup for field measurements at Houston, TX.

ACPD
13, 29413–29445, 2013

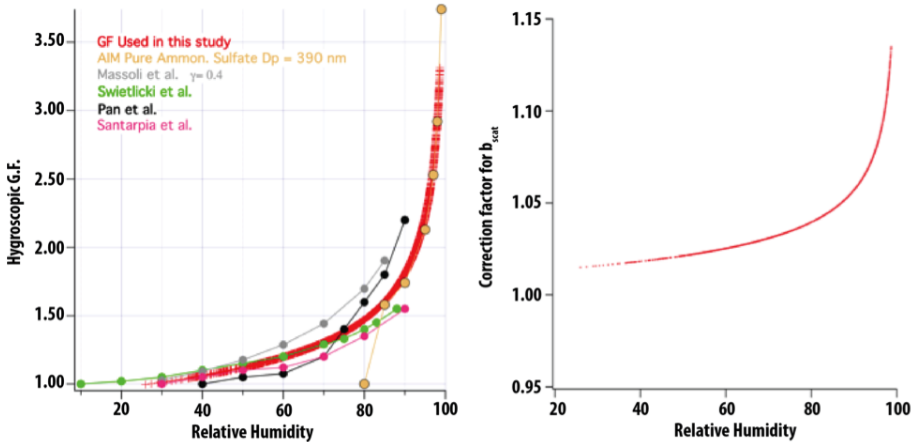

Fig. 2. Left – Hygroscopic growth factor (G.F.) model employed in this study (red) compared to select observational data from the literature (Pan et al., 2009; Swietlicki et al., 2008; Massoli et al., 2009; Santarpia et al., 2005) and predicted behavior for pure ammonium sulfate (Dp = 390 nm). Right – Correction factor for integrating sphere nephelometer derived from hygroscopic growth model and Qian et al. (2012). Scattering coefficients observed were corrected by this multiplier to account for angular truncation effects. Such a correction reduces observed absorption and M.A.C. values compared to the uncorrected case.

ACPD
13, 29413–29445, 2013

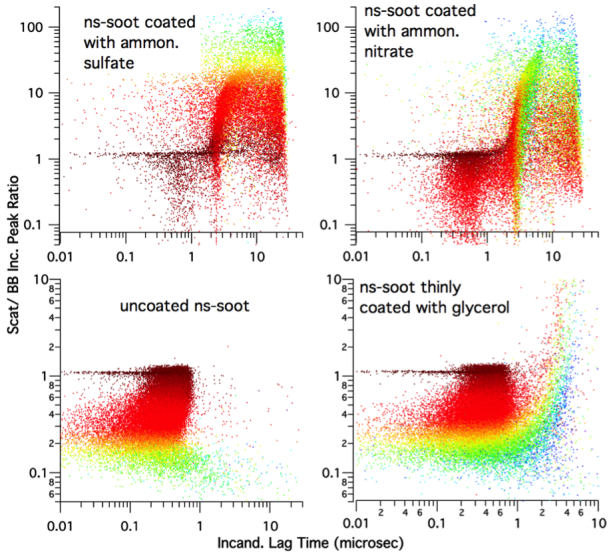

Fig. 3. Laboratory validation of lag time analysis to assess rBC mixing state. Data is for fresh, uncoated kerosene lamp soot and atomized kerosene lamp soot coated with ammonium sulfate, ammonium nitrate, and glycerol. For fresh, uncoated nanosphere soot (ns-soot) produced by a kerosene lamp the observed SP-2 lag time was < 1 µs for nearly all particles. However, lag time increased to > 1 µs when soot from the lamp was collected, and atomized from aqueous dispersions containing either glycerol, ammonium sulphate or ammonium nitrate. Thus, we have employed a 1 µs lag time delay as a criterion for assessing soot mixing state. Color scale indicates rBC particle indicated mass based on incandescence peak area.

ACPD
13, 29413–29445, 2013

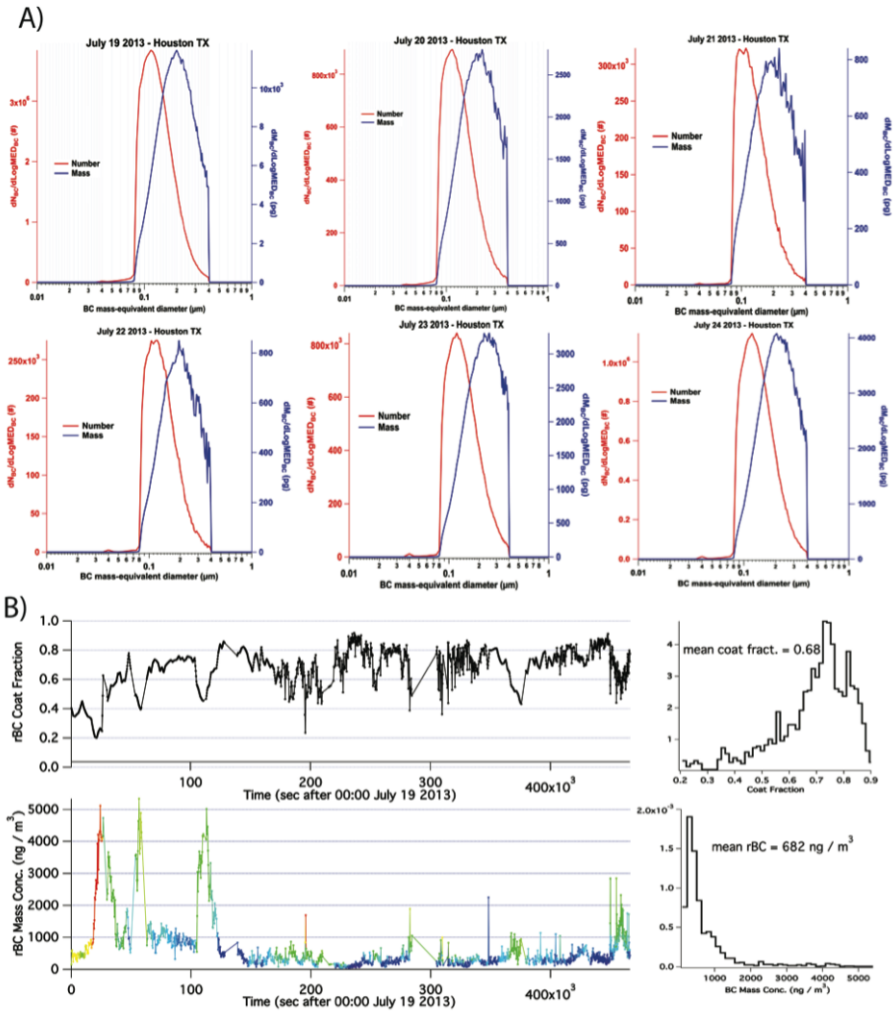

ACPD
13, 29413–29445, 2013

BC absorption at high RH

Y. Wei et al.

Fig. 4. (A) Daily average size distributions of rBC cores sampled at Houston, TX as reported by the SP2. Distributions were consistent from day-to-day with modes often near Dp = 120 nm. **(B)** Time series plot of BC coat fraction and mass concentration with histograms summarizing the data. The color scale corresponds to the BC coat fraction data. As observed, periods of high concentration of rBC often exhibited low coat fraction. Mean [BC] = 682 ng m^{-3} for the sampling period.

ACPD
13, 29413–29445, 2013

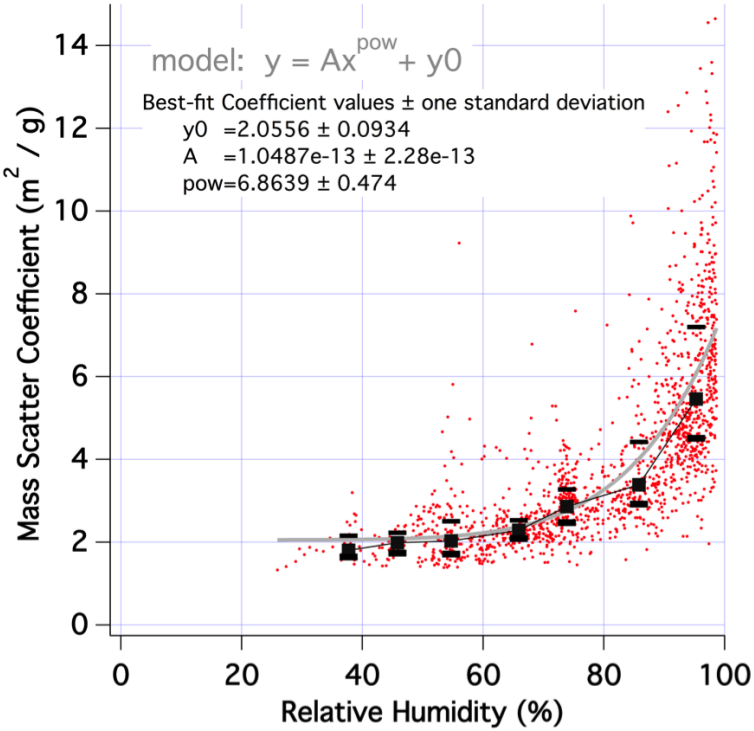

Fig. 5. Plot of observed mass scattering coefficient vs. relative humidity for aerosol sampled in Houston, TX during 19–24 July 2013. On average, scatter increases approx. 3-fold at high RH. The grey trace illustrates a best-fit to the power law relationship indicated. The black points represent the medians and 25–75th % tiles of measurements for data sorted into 10 % wide RH bins.

ACPD
13, 29413–29445, 2013

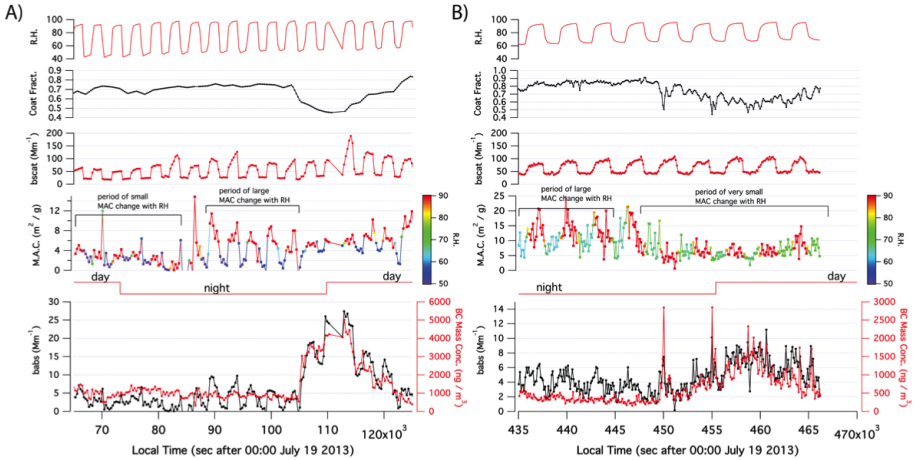

Fig. 6. Data collected during 19–24 July 2013 at Houston TX that exhibit rapid changes in observed absorption enhancement due to RH. In **(A)**, the initial 20 000 s exhibited small enhancement of MAC during periods of high RH – despite a large BC coat fraction. However between approx. 85–105 ks a very abrupt change in behavior was noted. Similar changes are observed in 6B at approx. 447 ks into the sampling period. In 4b the period of abrupt change corresponds with a drop in BC coat fraction. However, such a large drop in coat fraction was not observed in **(A)**. Results suggest the MAC of atmospheric soot and the enhancement at high RH is variable, and chemical composition of coatings may play significant role in the absorption enhancement process.

ACPD
13, 29413–29445, 2013

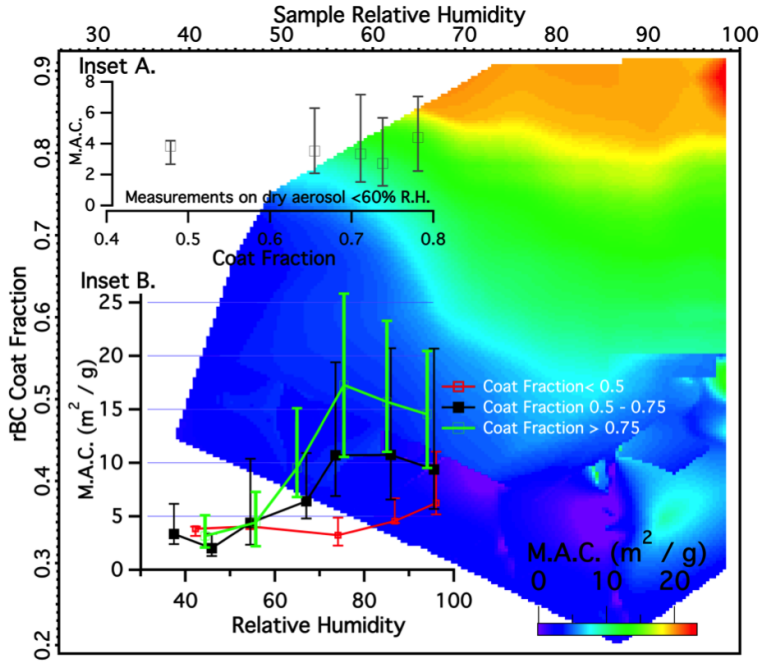

Fig. 7. Observed soot MAC at $\lambda = 532$ nm vs. RH and coating state for all data. The square data points in the plots represent medians of pooled points and error bars are the quartiles. Inset A plots observed M.A.C. values vs. coating state for dried aerosol (RH < 60 %). A slight increase in median from 3.8–4.4 $m^2 g^{-1}$ was observed as coating fraction increased. Inset B illustrates the dramatic increase in MAC when RH was > 60 %. The increase in M.A.C. was largest when the rBC coating fraction was high, suggesting additional coating materials increase hygroscopicity and lead to enhanced absorption by BC. Image plot was median filtered at 60 pixels. An uncertainty analysis is presented in Supplement S4.

ACPD
13, 29413–29445, 2013

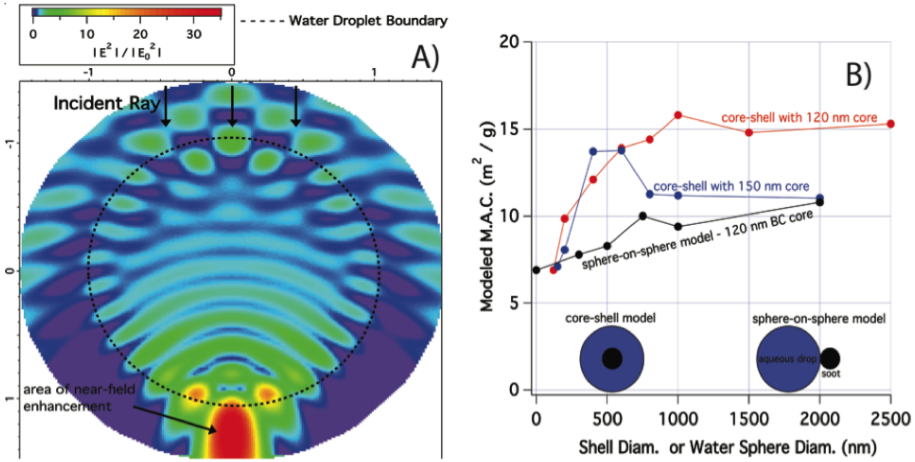

Fig. 8. (A) Modeled electric field within and near a 2 micron water droplet. The dashed line is the droplets boundary and x, y-axis are in micrometers. As observed, field enhancements are possible both within and immediately outside of the droplet. **(B)** Plot of modeled soot MAC vs. the shell diameter or water sphere diameter for the core-shell and sphere-on-sphere models. For the sphere-on-sphere model the BC core was always 120 nm. While the sphere-on-sphere model did produce an absorption enhancement, MAC values of 15 $m^2 g^{-1}$ were only possible for the core-shell model. Orientation averaging was employed for the sphere-on-sphere case.

ACPD
13, 29413–29445, 2013

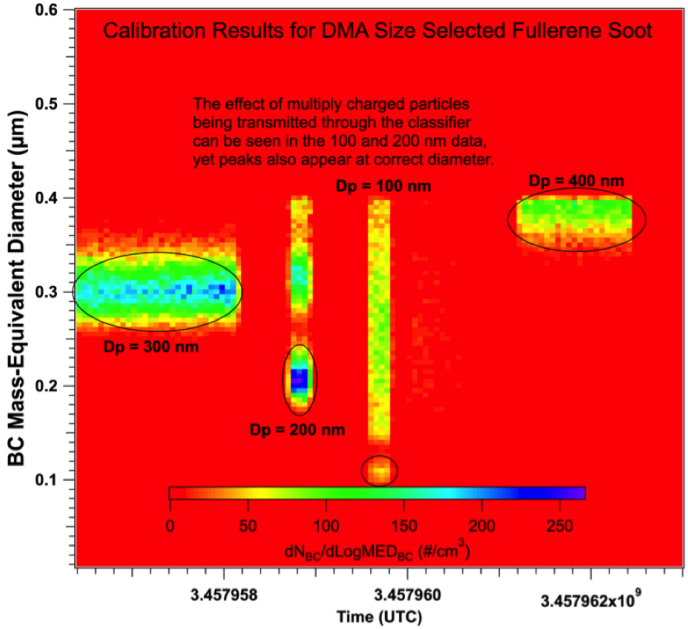

Fig. A1. Laboratory calibration of SP2 after the field campaign. Fullerene soot was atomized from an aqueous suspension and size selected to Dp = 100, 200, 300 or 400 nm with an electrostatic classifier. After calibration, the SP2 produced BC mass equivalent diameters identical to those expected and this calibration was applied to the Houston data. The effects of multiply charged particles being transmitted through the classifier are seen for the Dp = 100 nm and Dp = 200 nm cases, yet a peak in the distribution is still clearly visible at the desired diameter.

ACPD
13, 29413–29445, 2013

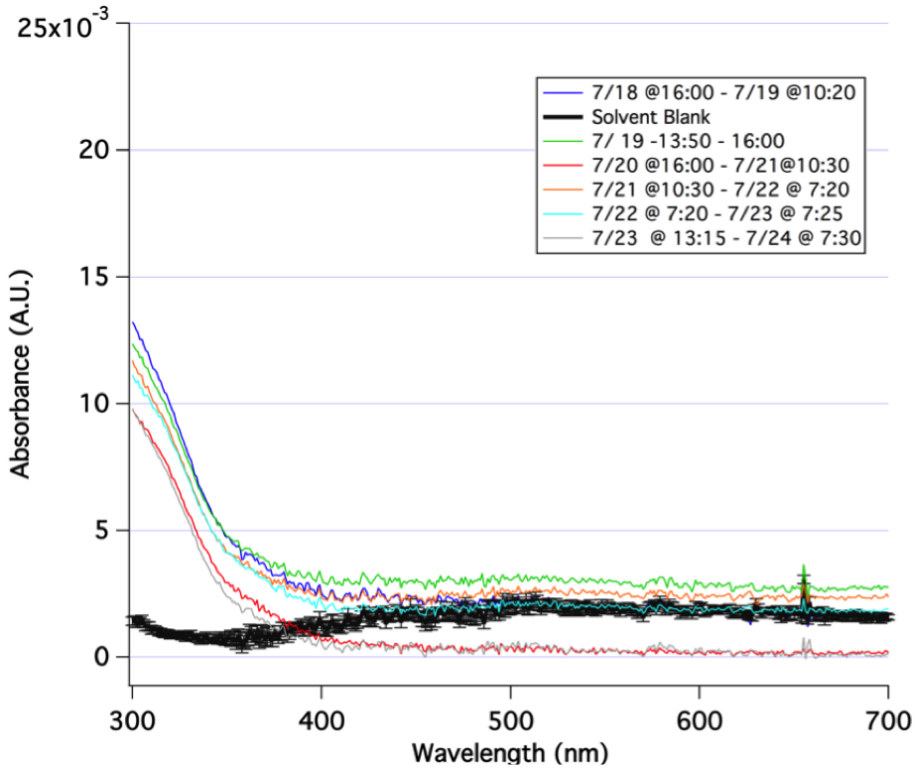

Fig. A2. Evaluation of possible "brown carbon" interference. UV-VIS Spectra of filter extracts collected from Houston, TX and a spectroscopic blank (black). Particles deposited onto a filter were extracted into 1.5 mL of 20 % methanol: 80 % water (v/v). Extracts were filtered through a 0.2 micron syringe filter prior to analysis. For reference, 4 mAU corresponds to a 1 % change in transmittance. The particle samples exhibited increased absorbance in the 300–400 nm spectral window, but the lack of significant visible absorption suggests brown carbon did not play a significant role in absorbing light for the samples considered. Times indicated are local.

ACPD
13, 29413–29445, 2013

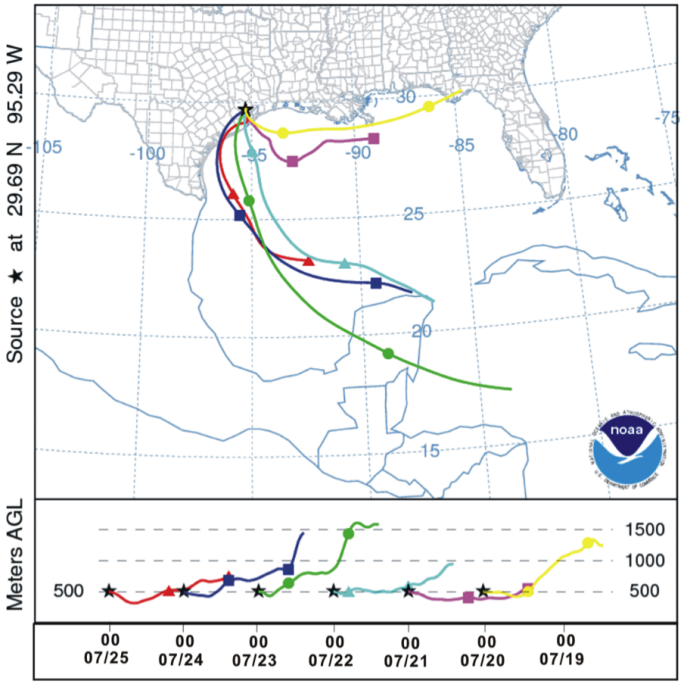

Fig. A3. NOAA HYSPLIT Back Trajectory Analysis during the sampling period. The authors gratefully acknowledge the NOAA Air Resources Laboratory (ARL) for the provision of the HYSPLIT transport and dispersion model and/or READY website (http://www.ready.noaa.gov) used in this publication.

ACPD
13, 29413–29445, 2013

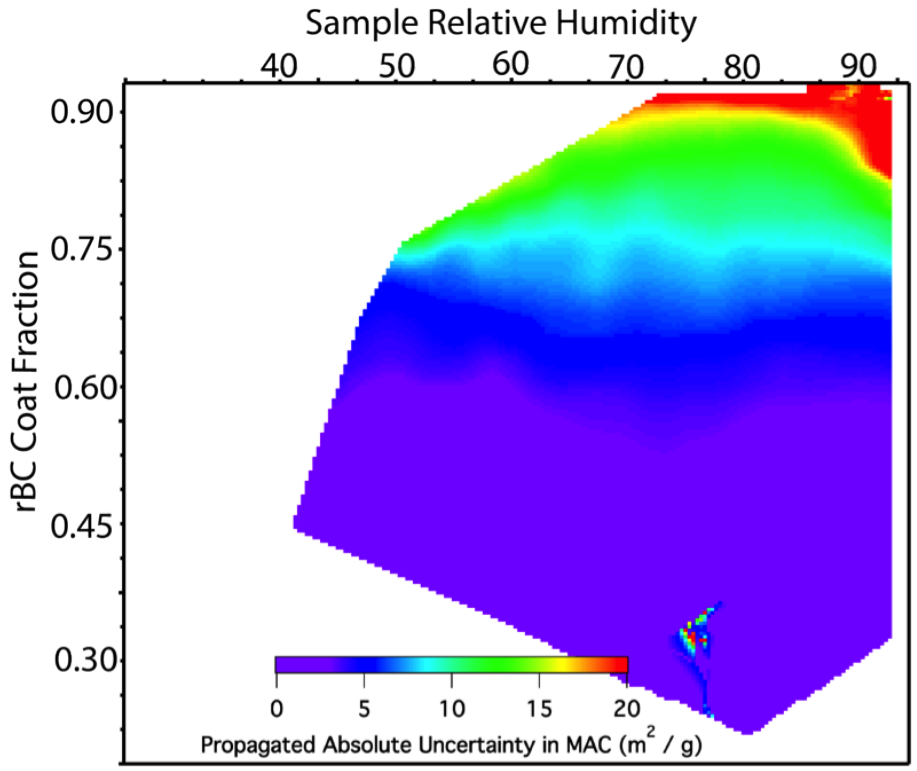

Fig. A4. Uncertainty analysis that accompanies Fig. 7 of this work. This figure presents propagated absolute uncertainty in MAC vs. coat fraction and RH. Because higher BC coat fractions were often observed when rBC mass concentration and b_{abs} were very low, the propagated absolute uncertainty in MAC is not constant. Highest absolute uncertainty was present at high rBC coat fractions, where largest MAC enhancement was also observed. For this analysis, an absolute uncertainty of b_{abs} = 2 Mm^{-1} and [BC mass] = 50 $ng\,m^{-3}$ were used. Uncertainty was propagated through the computation of MAC using the sum of squares of relative uncertainty approach.

ACPD
13, 29413–29445, 2013